Numerical Modelling of Injection Moulding: Comparisons using the Phan-Thien-Tanner & Criminale-Erickson-Fibley models

N.S. Hanspal, A. Kulkarni, A.N. Waghode & V. Nassehi*

Department of Chemical Engineering
Loughborough University
Loughborough, Leicestershire LE11 3TU
United Kingdom
a.kulkarni@lboro.ac.uk

ABSTRACT

Finite element technique is used to model the free surface flow regime representing injection mould filling of elastomeric material such as rubber compounds. The most distinct feature of the constitutive behaviour of elastomers, is the influence of material elasticity on the elongation and shear deformation suffered by the fluid during flow. In the present paper we tackle this effect by the use of Phan-Thien-Tanner (P-T/T) and Criminale-Erickson-Fibley (CEF) models. For the simple geometry used in the current work, the 2-D model for the representation of the flow is based on the Cauchy's and the continuity equation for an incompressible fluid. A continuous penalty/Galerkin finite element scheme is used for the solution of governing equations of the CEF model, whilst for the P-T/T model equations, a decoupled finite element scheme has been used. A scheme based on the Volume of Fluid technique is developed for free surface tracking. The solution of the free surface equation, which mainly represents the convection of free surface boundary in line with the flow, is based on the Stream Line Upwind Petrov Galerkin Scheme (SUPG). Time stepping used in conjunction with the two schemes is based on the well known Implicit-Theta method. Comparisons are made between the results obtained from both the models and their applicability to industrially relevant situations have been evaluated.

Keywords: Injection Moulding, CEF Model, P-T/T model, Front Tracking, VOF Technique, Finite Element Method

Email: a.kulkarni@lboro.ac.uk
Tel : +44 (0) 1509 222522
Fax : +44 (0) 1509 223923

INTRODUCTION

The rheological behaviours of elastomeric fluids are influenced by phenomena such as elongational deformation and shearing effects. The mathematical representations of these phenomena are relatively complex and their incorporation in the fluid flow equations is not straightforward. It has been reported that the Maxwell type constitutive equations for viscoelastic fluids do not provide acceptable solutions for processes such as injection moulding of rubber compounds (Tanner, 2000). Therefore, the modelling strategies developed for purely viscous flows obviously don't generate accurate numerical solutions to processes involving elastomers such as rubber compounds.

In addition to these rheological properties, there are some molecular level effects such as the possibility of the onset of preamature cross-linking rubber molecules at the free surface of flow front entering the injection mould. These cross-linkings will cause hardening of the flow front progressing in the mould thereby creating hurdles for the flow. Such cross-linkings may even change the material properties of the bulk fluid. For these obvious reasons, the simulation of rubber moulding has not been deliverered a serious attention in the past despite the widespread work carried out on computational modelling of thermoplastics' mouldings (Isayev, 1991). The premature short cross-linking may lead to formation of cavities and gaps in the moulded compound causing obstructions to the flow.

In the present work, we have presented a computational model for the injection moulding of rubber compounds, based on the finite element numerical technique. The elongational and shear effects of the elatomeric rubber compound have been accounted by two different rheological constitutive models, namely Phan-Thien/Tanner equation (Phan-Thien and Tanner, 1977) and the Criminale-Erickson-Fibley equation (Bird *et al.*, 1987). In both the cases, the progression of the flow front in the injection mould has been estimated by a robust and generic moving boundary tracking scheme. The simulated results generated using both the constitutive relationships have been compared for their accuracy towards the retention of the history of deformation. It is shown that the developed computational algorithm has the capabilities to be used as a cost-effective design and simulation tool for the injection moulding of rubber compounds, accompanying the appropriate procedures. This model can be further utilised for the cross-examination of the effects related to change in the material properties of the bulk fluid in the mould. A brief discussion of the governing equations of the present model and an outline of the developed solution strategy are presented in the next section.

GOVERNING MODEL EQUATIONS USED IN PRESENT WORK

Using a two-dimensional coordinate system (x, y) the main model equations consist of the mass continuity for incompressible fluids given as

$$\frac{\partial V_x}{\partial x}+\frac{\partial V_y}{\partial y}=0 \qquad \textbf{(1)}$$

and the equation of motion for non-Newtonian fluids which in the absence of body forces is written as (Cauchy's equation of motion)

$$\begin{cases} \rho\left(\dfrac{\partial V_x}{\partial t}+V_x\dfrac{\partial V_x}{\partial x}+V_y\dfrac{\partial V_x}{\partial y}\right)=-\dfrac{\partial P}{\partial x}+\dfrac{\partial \tau_{xx}}{\partial x}+\dfrac{\partial \tau_{yx}}{\partial y} \\ \rho\left(\dfrac{\partial V_y}{\partial t}+V_x\dfrac{\partial V_y}{\partial x}+V_y\dfrac{\partial V_y}{\partial y}\right)=-\dfrac{\partial P}{\partial y}+\dfrac{\partial \tau_{xy}}{\partial x}+\dfrac{\partial \tau_{yy}}{\partial y} \end{cases} \qquad \textbf{(2)}$$

where V_x and V_y are the components of the velocity field, ρ is the fluid density, *P* is the pressure and τ_{xx} etc. are the components of the extra stress tensor. For purely viscous fluids (i.e. generalised Newtonian fluids) which do not exhibit significant elongational behaviour, it is possible to relate explicitly the components of the stress appearing in the equation of motion to the rate of strain (or deformation) within the fluid. This results in the elimination of the stress components from the equation of motion. However, for highly elastic fluids such as rubber this is not possible and in order to take into account the true constitutive behaviour of such fluids implicit relationships between the stress and the rate of strain components should be used. In the present work, we have used the CEF and P-T/T viscoelastic flow models in conjunction and decoupled FEM scheme respectively. The stresses appearing in equation (2) are related to the rate of strain tensor by equation (3).

$$\begin{cases} \tau_{xx}=2\eta\dfrac{\partial V_x}{\partial x}+(\psi_{12}+\psi_{23})\left[\dfrac{\partial V_x}{\partial y}+\dfrac{\partial V_y}{\partial x}\right]^2 \\ \tau_{yy}=2\eta\dfrac{\partial V_y}{\partial y}+\psi_{23}\left[\dfrac{\partial V_x}{\partial y}+\dfrac{\partial V_y}{\partial x}\right]^2 \\ \tau_{xy}=\eta\left[\dfrac{\partial V_x}{\partial y}+\dfrac{\partial V_y}{\partial x}\right] \end{cases} \qquad \textbf{(3)}$$

where η is shear viscosity given by the power-law model as $\eta=\eta^o\left(\dot{\gamma}\right)^{n-1}$, where, η^o is the material consistency coefficient, n is the power-law index and $\dot{\gamma}$ is the shear rate given by

$$\dot{\gamma}=\left\{2\left(\frac{\partial V_x}{\partial x}\right)^2+2\left[\left(\frac{\partial V_y}{\partial y}\right)^2+\left(\frac{\partial V_x}{\partial y}+\frac{\partial V_y}{\partial x}\right)^2\right]\right\}^{\frac{1}{2}} \qquad \textbf{(4)}$$

ψ_{12} and ψ_{23} are the empirical coefficients given by

$$\begin{cases} \psi_{12} = A\eta^{b}\left(\frac{1}{2}I_2\right)^{\left(\frac{b-2}{2}\right)} \\ \psi_{23} = \frac{1}{10}\psi_{12} \end{cases} \quad (5)$$

where A and b are two characteristic constants of a elastomer and I_2 is the second invariant of the rate deformation tensor.

The constitutive equations representative of the P-T/T Model (Phan-Thien & Tanner,1997) are given by set (6)

$$\begin{aligned}
&\lambda\left(\frac{\partial \tau_{xx}}{\partial t}+V_x\frac{\partial \tau_{xx}}{\partial x}+V_y\frac{\partial \tau_{xx}}{\partial y}\right)-2\lambda\left((1-\xi)\frac{\partial V_x}{\partial x}\tau_{xx}+\left(\frac{\partial V_x}{\partial y}-\frac{\xi}{2}\left(\frac{\partial V_x}{\partial y}+\frac{\partial V_y}{\partial x}\right)\right)\tau_{xy}\right)\\
&+\left(\left(1+\frac{\varepsilon\lambda}{\eta^o}\left(\tau_{xx}+\tau_{yy}\right)\right)\right)\tau_{xx}=2\eta\frac{\partial V_x}{\partial x}\\
&\lambda\left(\frac{\partial \tau_{xy}}{\partial t}+V_x\frac{\partial \tau_{xy}}{\partial x}+V_y\frac{\partial \tau_{xy}}{\partial y}\right)-\lambda\left(\frac{\partial V_x}{\partial y}-\frac{\xi}{2}\left(\frac{\partial V_x}{\partial y}+\frac{\partial V_y}{\partial x}\right)\right)\tau_{yy}-\lambda\left(\frac{\partial V_y}{\partial x}-\frac{\xi}{2}\left(\frac{\partial V_x}{\partial y}+\frac{\partial V_y}{\partial x}\right)\right)\tau_{xx}\\
&+\left(\left(1+\frac{\varepsilon\lambda}{\eta^o}\left(\tau_{xx}+\tau_{yy}\right)\right)\right)\tau_{xy}=\eta\left(\frac{\partial V_x}{\partial y}+\frac{\partial V_y}{\partial x}\right)\\
&\left(\frac{\partial \tau_{yy}}{\partial t}+V_x\frac{\partial \tau_{yy}}{\partial x}+V_y\frac{\partial \tau_{yy}}{\partial y}\right)-2\lambda\left(\begin{array}{l}(1-\xi)\frac{\partial V_y}{\partial y}\tau_{yy}+\\ \left(\frac{\partial V_y}{\partial x}-\frac{\xi}{2}\left(\frac{\partial V_x}{\partial y}+\frac{\partial V_y}{\partial x}\right)\right)\tau_{xy}\end{array}\right)+\left(\left(1+\frac{\varepsilon\lambda}{\eta^o}\left(\tau_{xx}+\tau_{yy}\right)\right)\right)\tau_{yy}=2\eta\frac{\partial V_y}{\partial y}\\
&\lambda\left(\frac{\partial \tau_{yy}}{\partial t}+V_x\frac{\partial \tau_{yy}}{\partial x}+V_y\frac{\partial \tau_{yy}}{\partial y}\right)-2\lambda\left(\begin{array}{l}(1-\xi)\frac{\partial V_y}{\partial y}\tau_{yy}+\\ \left(\frac{\partial V_y}{\partial x}-\frac{\xi}{2}\left(\frac{\partial V_x}{\partial y}+\frac{\partial V_y}{\partial x}\right)\right)\tau_{xy}\end{array}\right)+\left(\left(1+\frac{\varepsilon\lambda}{\eta^o}\left(\tau_{xx}+\tau_{yy}\right)\right)\right)\tau_{yy}=2\eta\frac{\partial V_y}{\partial y}
\end{aligned} \quad (6)$$

where, λ is the relaxation time and ξ is a characteristic elongation parameter $(0 \le \xi \le 2)$(Nassehi,2002).

MODELLING SCHEME

To solve the equations of the P-T/T model, we have used a de-coupled solution scheme. In this approach the simulation cycle starts with the solution of Stokes (i.e. Newtonian) equations for incompressible fluids. This solution yields the first set of velocity and pressure fields that can be inserted into the P-T/T equation to obtain the viscoelastic stress components. Stress gradients are in turn found and inserted into the Cauchy's equation and new velocity and pressure fields are computed. The cycle consisting of the solution of the P-T/T and Cauchy's is iterated until convergence is achieved. Time variable is

then incremented and the cycle is repeated till the predetermined end of simulation. Solution of the Stokes flow equations at the start of the simulation is based on the continuous penalty/ Galerkin finite element scheme which combines efficiency with computing economy (Nassehi, 2002). A similar scheme is used to solve the Cauchy's equation of motion. The velocity field obtained using the continuous penalty scheme provides the necessary data for generating the pressure field via the variational recovery method (Pittman and Nakazawa, 1984). The variational recovery method is also used to calculate gradients of all field variables (e.g. stress gradients) at computational nodes. The solution of the free surface equation, which mainly represents the convection of free surface boundary in line with the flow, is based on the Stream Line Upwind Petrov Galerkin (SUPG) scheme (Nassehi, 2002). This equation is solved at the end of each time step after converged values for the velocity are found to determine the position of the free front. Details of the derivation of the working equations of the described scheme are published previously (Hou and Nassehi, 2001) and will not be repeated here.

On the contrary, for the solution of CEF model equations continuous penalty/Galerkin finite element scheme which combines efficiency with computing economy (Nassehi,2002) has been used. The cycle consisting of the computation of field variables is iterated until convergence is achieved. Time variable is then incremented and the cycle is repeated till the predetermined end of simulation. The velocity field obtained using the continuous penalty scheme provides the necessary data for generating the pressure field via the variational recovery method (Nassehi,2002). For capturing the mould flow front, the solution of free surface equation is determined exactly in the same manner as described for the P-T/T model summarised above. The final finite element working equation of the CEF model can be referred in Hanspal *et al* (2005). The time-stepping scheme used in conjunction with both the P-T/T and CEF models is based on the well known implicit θ method (Nassehi,2002). The main focus of the present study has been the front tracking of free surface flows, which is the dominant factor in the simulation of mould filling processes.

FREE SURFACE TRACKING

The advancing flow front within the mould is simulated using the VOF (volume of fluid) technique. This method is based on the solution of the surface position probability density equation, given as

$$\frac{\partial F}{\partial t} + V_x \frac{\partial F}{\partial x} + V_y \frac{\partial F}{\partial y} = 0 \qquad \textbf{(7)}$$

where $0 \le F \le 1$ is called the surface position function. In this work we have used a modified version of the VOF technique in which the moving boundary flow regime is considered as a two-phase regime in which the filled and the voids (air filled) sections are considered as different phases (Thompson,1986). The flow model is solved for the entire domain whilst at each section physical properties relevant to that phase are inserted. Simultaneous solution of equation (3) with the flow model generates values of

F . A value of *F* between 0 and 1 (usually $F = 0.5$) is taken as the boundary between phases representing the moving free surface. Values of physical parameters for each phase in the flow field is related to the position of the free surface using the following equation

$$y = y_f F + y_a (1 - F) \tag{8}$$

where y is a given physical parameter and y_f and y_a are the values of this parameter in the fluid and air filled regions, respectively, (Nassehi and Ghoreishy, 1997).

FINITE ELMENT DISCRETIZATION OF THE FREE SURFACE EQUATION AND SOLUTION SCHEMES

We have used the weighted residual finite element method to derive the working equations corresponding to the free surface position function. In this procedure the inner product of equation (7) and a suitable weight function is constructed as

$$\langle \dot{F}, \hat{\psi}_i \rangle + \overline{V} \bullet \nabla F, \hat{\psi}_i \rangle = 0 \tag{9}$$

where $\hat{\psi}_i$ represents streamlined upwind weight function given as

$$\hat{\psi}_i = \varphi_i + \gamma_c \frac{\left| h_x V_x + h_y V_y \right|}{2\left|\overline{V}\right|^2} \left(V_x \frac{\partial \varphi_i}{\partial x} + V_y \frac{\partial \varphi_i}{\partial y} \right) \tag{10}$$

where φ_i is the normal Galerkin weight function which is identical to the shape functions used to represent elemental approximation of the function *F* as $\widetilde{F} = \sum_{j=1}^{p} F(j)\varphi_j$, *p* is the number of nodes per element, $0 < \gamma_c \geq 1$ is the upwiding constant , and h_x and h_y are characteristic lengths given as

$$h = \sqrt{(h_x)^2 + (h_y)^2} = \sqrt{\left(\frac{\partial x}{\partial \xi} + \frac{\partial x}{\partial \eta} \right)^2 + \left(\frac{\partial y}{\partial \xi} + \frac{\partial y}{\partial \eta} \right)^2} \tag{11}$$

where (ξ, η) is a elementally defined co-ordinate system. Within the space of a finite element after substitution of function *F* with approximate representation in terms of elemental shape functions equation (4) is written as

$$\int_e [\sum_{j=1}^{p} \dot{F}_j \varphi_j + \left(V_x \frac{\partial}{\partial x} F_j \varphi_j + V_y \frac{\partial}{\partial y} F_j \varphi_j \right)] \hat{\psi}_i dx dy = 0 \quad i = 1,..p \tag{12}$$

Using matrix notation

$$[M]\{\dot{F}\}+[K]\{F\}=0 \quad \textbf{(13)}$$

where $[M]$ and $[K]$ are the mass and stiffness matrices, respectively. After the time stepping of equation (5), via the θ method (Nassehi, 2002), the required working equation is obtained as

$$([M]+\theta\Delta t[K])\{F\}_{n+1}=([M]-(1-\theta)\Delta t[K])\{F\}_n \quad \textbf{(14)}$$

where Δt and n represent time increment and time step, respectively.

The solution algorithms used for the free surface tracking schemes in conjunction with the CEF and P-T/T models can be found in Hanspal *et al*. (2005) and Ali & Nassehi (2002) respectively.

COMPUTER SIMULATIONS

The mould used to study these effects is of a two-plate design whose schematic diagram is shown in figure1. The feed system for this mould consists of a sprue connected to a U shaped runner, which ends at a diverging gate. The material is injected through sprue at a constant flow rate using an injector. The injector is a displacement device, which is designed to maintain a steady flow rate entering into the runner through the sprue. The injection continues until the mould is filled. The input data used in the present simulations are:

Physical data

Fluid density = 1055 kg m^{-3}, consistency coefficient = 88700 kg $m^{-1}s^{-1}$, power law index = 0.20, density of air = 1.2929 kg m^{-3}, viscosity of air = $0.251\text{x}10^{-4}$ Pa s. The values of A and b used in the CEF model i.e. characteristic constants of elastomer are 0.00347 and 1.66, respectively.

Initial and Boundary conditions

Initial velocity=0, everywhere. Inlet velocity=0.1ms^{-1} (corresponding to a constant volumetric flow rate) and no slip at solid walls has been assumed.

Data used in the finite element scheme

Penalty parameter $\lambda = 10^{10}$, Time increment Δt = 0.01667 s. Initially, the flow domain is discretised into 1100 nine noded C^0 bi-quadratic finite elements and the convergence of the solutions is checked via mesh refinement by doubling the number of elements after the initial run.

The mould filling operation considered here takes 14.28 s in total. Choosing a time increment of 0.01667 s the process is simulated through nearly 857 steps. In the following figures simulated flow front within the modelled mould cavity obtained at various time steps are shown. Accuracy of the simulations is checked by comparing amount of fluid entered into the mould with the fluid injected through the sprue at a steady rate. The amount of fluid entering the mould can be found by measuring the extent of the advancement of the flow front.

Simulations have been carried, for both the CEF and P-T/T models with the air being assumed to be incompressible. The sample results show the advancement of the free surface boundary, which is tracked using the described algorithm. The flow fronts for the both the models considered have been presented at 4 different time steps, i.e.

Time step 200, corresponding to 3.3 s
Time step 400, corresponding to 6.7 s
Time step 600, corresponding to 10.0 s
Time step 800, corresponding to 13.3 s

All the results have been validated by performing mass balance checks based on the Cartesian coordinate system for the geometry shown in figure 1.

In figure 2, the advancement of the front is presented for a CEF model. It can be seen that the front boundary at all the time levels is not exactly symmetric. The fluid retains its memory of asymmetric deformation within the runner and exhibits a behaviour because reflecting viscoelastic nature of the CEF model equations. As seen in the figure, with the advancement of the fluid front in the mould the asymmetry gradually diminishes, the fluid tends to loose its memory and relaxes which is visible from the shape of front at time 13.33 s. This case was also analysed when air was assumed to be compressible and the geometry of the front advancement was found to be negligibly different from the incompressible case. In an actual mould there will be little holes for the air to escape. Therefore, by assuming the air to be incompressible simulations become closer to reality. A direct comparison has also been made between the results obtained from CEF model and Phan-Thein/Tanner model. The results for the Phan-Thein/Tanner model, are shown in figure 3, were computed by using a de-coupled continuous penalty scheme in which the Cauchy's equation of motion and Phan-Thein/Tanner viscoelastic model equations were solved separately. The solution of the free surface equation, which represents the convection of free surface boundary in line with the flow, is based on the Stream Line Upwind Petrov Galerkin (SUPG) scheme. The front profiles obtained from the Phan-Thein/Tanner model appear to be random and cannot be interpreted by theoretical analysis. However, these results should be treated cautiously for the following reasons.

Accurate measurement of the rheological parameters such as elongation viscosity and relaxation time appearing in the Phan-Thein/Tanner constitutive equation is not a trivial matter. This poses a severe restriction on the reliability of the simulation results obtained using this model. In the present work a set of values reported in the literature are used (Clarke & Petera, 1997). Secondly, we suspect that solution of the Phan-Thein/Tanner constitutive model equations in conjunction with free surface tracking may involve some errors due to the upwinding used to solve both equations in an Eulerian framework. Such errors diminish significantly using a simpler constitutive equation such as CEF. Considering these factors, and in view of the fact that the results obtained by the CEF model appear to be logical and in line with the theoretical expectations, it was decided to abandon any further simulation of the mould filling problem presented here using the Phan-Thein/Tanner model. The inclusion of the results obtained by this model is only to show that ad hoc use of a more sophisticated viscoelastic constitutive model may in fact lead to errors rather than improving simulations quality.

CONCLUSIONS

The developed finite element scheme is shown to generate useful simulations for the mould filling process. CEF model represents a more realistic viscoelastic behaviour of elastomeric fluid being modelled and stable numerical results are generated without excessive computational cost. The observed asymmetry of the flow front in the results is in accordance with the normal behaviour of a memory fluid. Such a fluid is expected to demonstrate an uneven deformation on its parts during the flow through the U shaped runner modelled in the present study. Overall, the results are self-consistent and provide useful data for further analysis of the mould filling process. The work is now being extended to examine the effect of cross linking of rubber chains on the free surface by comparing the above results with simulations obtained using material data for cross linked rubber within elements located at the flow front.

NOMENCLATURE

A	Characteristic constant of the elastomer
b	Characteristic constant of the elastomer
F	Free surface position
I_2	Second invariant of rate of deformation tensor
dn_x	Component of the unit normal vector in the *x* direction
dn_y	Component of the unit normal vector in the *y* direction
n	Power law index
N_i	Elemental shape function/ weight function
$\tilde{p}$	Interpolated form of pressure
P	Pressure
V_x	*x* component of the velocity
V_y	*y* component of the velocity
V_x^*	*x* component of the velocity at previous time step
V_y^*	*y* component of the velocity at previous time step
$\tilde{V}_x$	Interpolated form of the *x* component of the velocity vector
$\tilde{V}_y$	Interpolated form of the *y* component of the velocity vector
t	Time variable

GREEK SYMBOLS

λ	Relaxation time
ξ	Characteristic Elongation parameter
η	Viscosity of the fluid
η^0	Material consistency coefficient
Ω	Solution domain
Ω_e	Element domain
ρ	Fluid density
η_0	Consistency coefficient used in power law
$\dot{\gamma}$	Shear Rate
•	Boundary of the solution domain
$•_e$	Elemental boundary
•	Time stepping parameter
ψ_{12}	Empirical coefficient for the elastomer
ψ_{23}	Empirical coefficient for the elastomer
τ_{xx}	Component of the stress tensor
τ_{xy}	Component of the stress tensor
τ_{yx}	Component of the stress tensor
τ_{yy}	Component of the stress tensor

REFERENCES

Bird, R.B., Armstrong, R.C. and Hassanger, O. 1987. Dynamics of polymeric fluids, fluid mechanics, Vol. 1, Wiley, New York.

Clarke, J. and Petera., J. 1997. Determination of steady state elongational viscosity for rubber compounds using bell mouth dies, *J. Applied Polymer Sciences*, Vol. 66, 1139.

Hanspal, N.S., Nassehi, V.N. and Ghoreishy, M.H.R. 2005. "Simulation of Rubber Moulding Using Finite Element Modelling", *International Journal of Polymer Processing*, Vol. 20, 3.

Hou, L. and Nassehi, V. 2001. Evaluation of stress-effective flow in rubber mixing, Nonlinear Analysis, Vol. 47, 1809.

Isayev, A.I. 1991. Modelling of Polymer Processing, Hanser Publisher, Munich.

Nassehi, V. and Ghoreishy, M.H.R. 1997. Simulation of free surface flow in partially filled internal mixers, *International Polymer Processing*, Vol.12, 346.

Nassehi, V. 2002. Practical Aspects of Finite Element Modelling of Polymer Processing, John Wiley and Sons, Chichester.

Nassehi, V.N. and Ali, B. 2002. Simulation of Rubber Moulding using Finite Element Moulding, *Industrial Simulation Conference*, Valencia, Spain.

Phan-Thien, N. and Tanner., R.I. 1977. A New Constitutive Equation Derived From Network Theory, *J. Non-Newtonian Fluid Mech*. Vol. 2, 353.

Pittman, J.F.T.; and S. Nakazawa. 1984. Finite Element Analysis of Polymer Processing Operations. In: Pittman, J.F.T., Zienkiewicz, O.C., Wood, R.D. and Alexander, J.M., Numerical Analysis of Forming Process. John Wiley and Sons, Chichester.

Tanner, R.I. 2000. Engineering Rheology, 2nd Ed. Oxford University Press, Oxford.

Thompson, E. 1986. Use of Pseudo-concentration to follow creeping flows during transient analysis, *Int. J. Numer. Methods Fluids*. Vol. 6, 749.

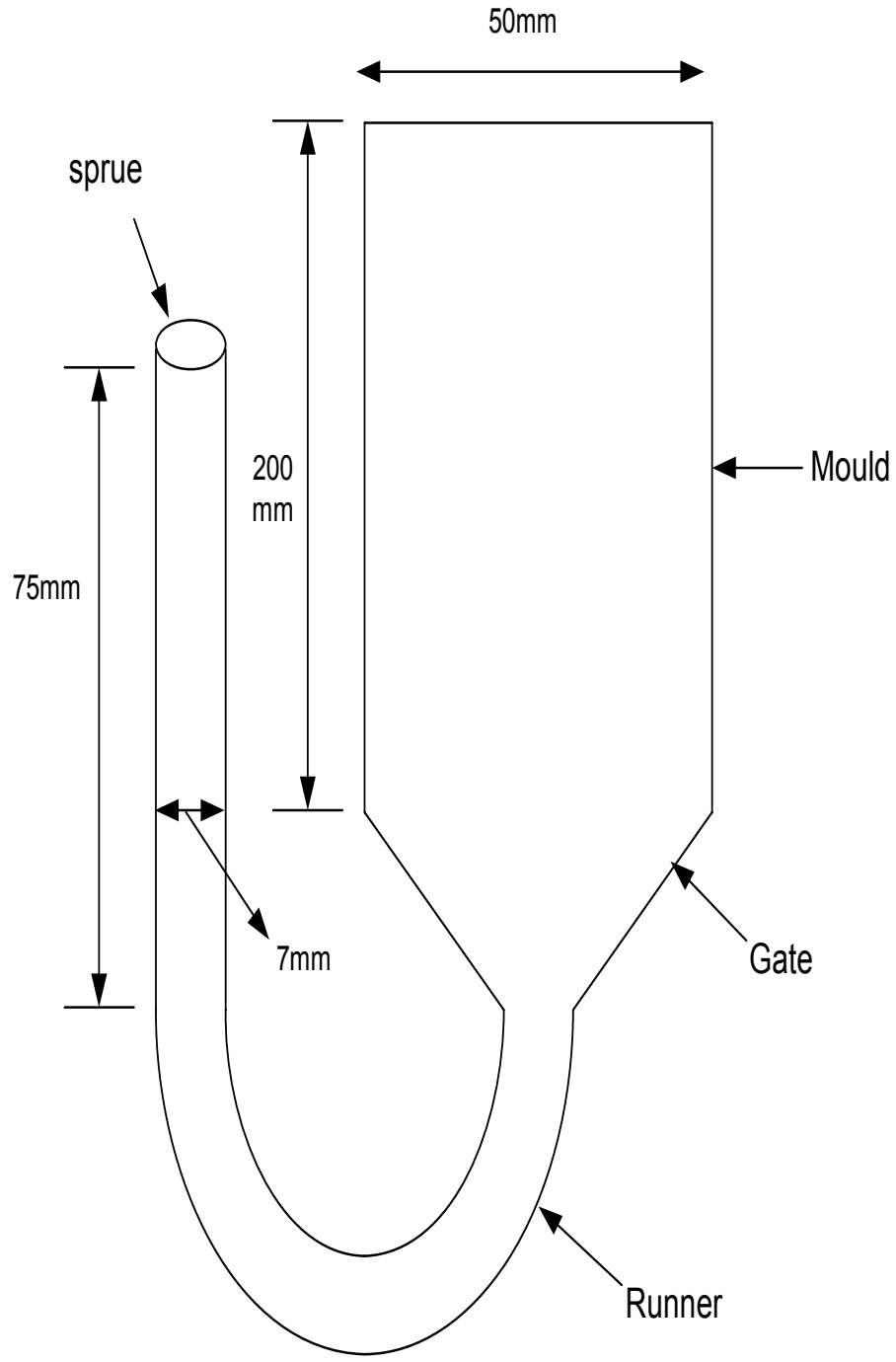

Figure 1: SCHEMATIC DIAGRAM OFINJECTION MOULDING PROCESS SIMULATED HERE

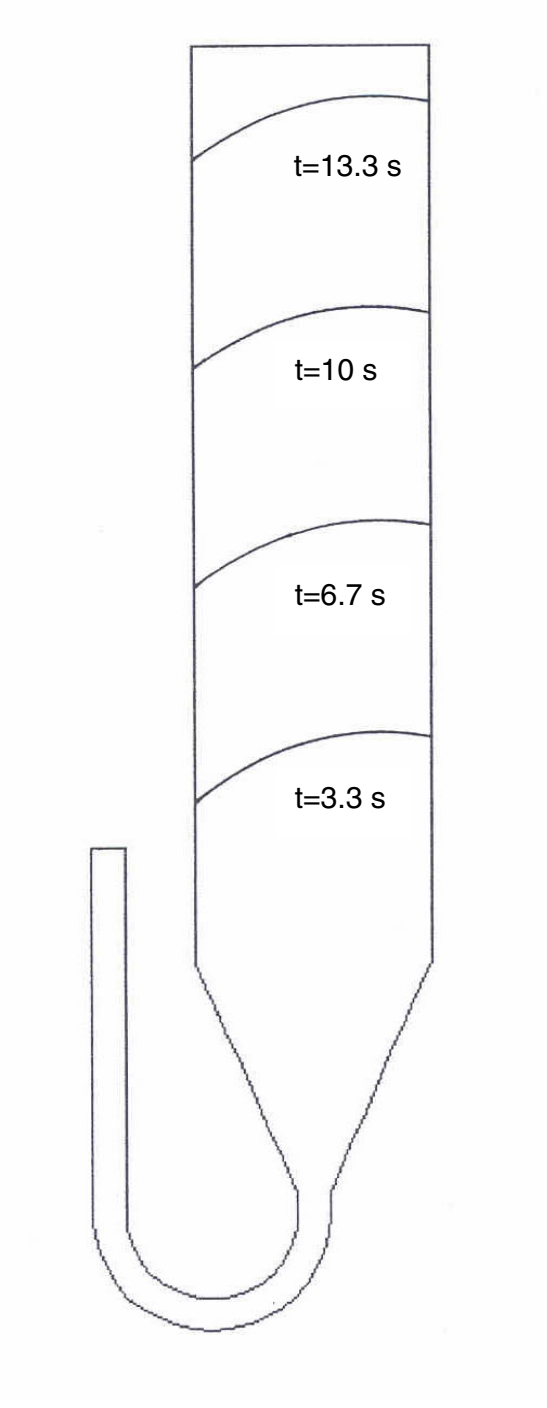

Figure 2: PREDICTED FLOW FRONTS FOR CEF MODEL

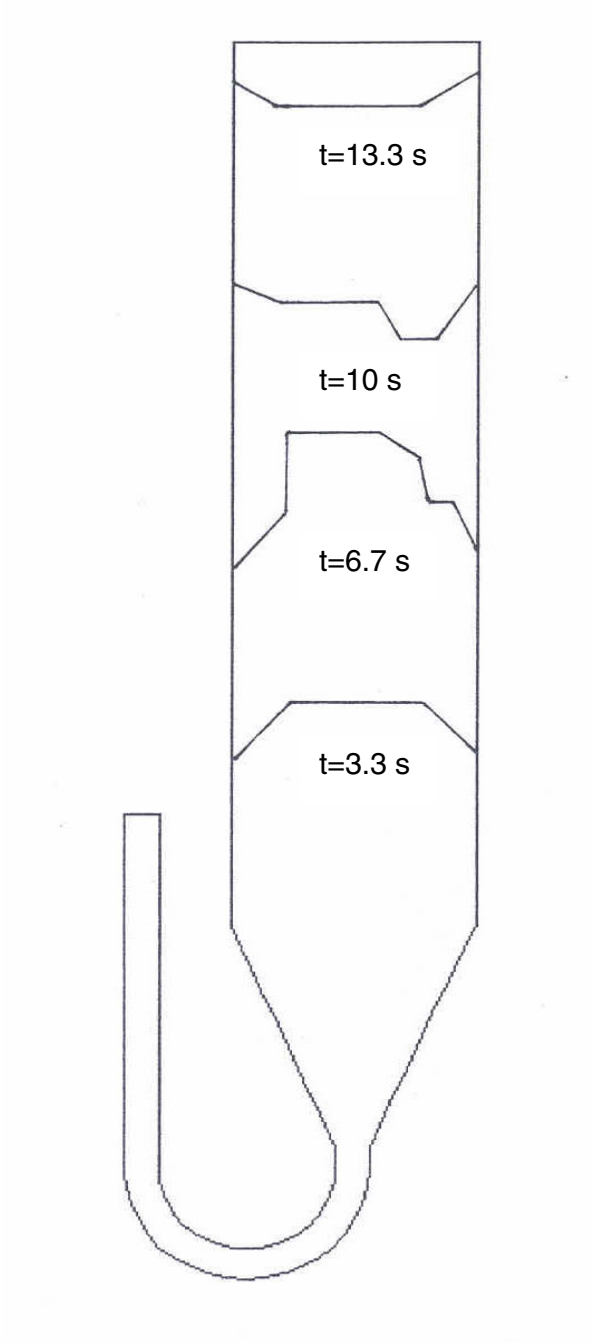

Figure 3: PREDICTED FLOW FRONTS FOR THE PHAN-THIEN/TANNER MODEL